8.3 ERROR ANALYSES AND TESTS
OF PRESSURE-GRADIENT FORCE SCHEMES IN A NONHYDROSTATIC, MESOSCALE MODEL

Dave Dempsey**
San Francisco State University
San Francisco, CA

Chris Davis
National Center for Atmospheric Research*
Boulder, CO

## 1. INTRODUCTION

Expressed in terrain-following (σ) coordinates, the horizontal pressure-gradient, $\nabla_H p$, comprises two terms: $\nabla_\sigma p + \nabla_H \sigma(\partial p/\partial\sigma)$. The first term represents the rate of variation in pressure along a σ-surface, while the second term compensates for vertical variations inherent in the first term. These terms tend to be largest over steep terrain near the surface, where σ-surfaces slope most steeply. As has been understood for decades, inconsistent discretization of these terms can fail to account properly for the partial compensation between them, producing errors in estimates of the horizontal pressure-gradient force (PGF).

Historically, such errors have attracted attention in hydrostatic models, where consistency with the discretization of the hydrostatic equation is an issue and where vertical variations in pressure vastly exceed horizontal variations, and to models in which full pressure, rather than perturbation pressure, is discretized. However, the same problem arises in principle (if not necessarily in severity) in nonhydrostatic models formulated in terms of perturbations relative to a hydrostatic basic state.

To investigate the potential severity of compensation errors in the PGF term, and the ability of alternative PGF schemes to minimize those errors, we have (1) performed formal truncation error analyses of a common PGF discretization scheme, plus a number of alternatives; and (2) designed idealized simulations to test PGF schemes the Penn State-NCAR nonhydrostatic mesoscale model (MM5) (Dudhia, 1993). Similar analyses should apply to models formulated in terms of geopotential height or Exner function.

*The National Center for Atmospheric Research is sponsored by the National Science Foundation.

**Corresponding author address: Dr. Dave Dempsey; Dept. of Geosciences, SFSU; 1600 Holloway Ave.; San Francisco, CA 94132
email: ddempsey@sundog.sfsu.edu

## 2. THE "STANDARD" PGF SCHEME

Dempsey (1996) showed that, like the "standard" PGF discretization schemes in many models, MM5's PGF scheme in effect (1) vertically extrapolates pressures on each side of a velocity point from a σ-surface to a horizontal surface containing the velocity point; and (2) differences the extrapolated pressures to estimate the horizontal PGF at the velocity point.

Fig. 1 helps illustrate the standard PGF scheme on a staggered grid in two dimensions. In Fig. 1, the quantity $(\partial z_s/\partial x)/(\Delta z/\Delta x)$ (where $\partial z_s/\partial x$ is the terrain slope and Δz and Δx are the vertical and horizontal grid resolutions, respectively) is relatively large, as it might be near the surface of steep terrain with a high-resolution PBL scheme, for example. Regardless of the context, to estimate $\hat{p}_{j+1,k}$, the standard PGF scheme in effect (1) estimates the height, $z_{j+1/2,k}$, of the velocity point $u_{j+1/2,k}$; and (2) extrapolates p linearly w/r/t σ from $p_{j+1,k}$ to level $z_{j+1/2,k}$, using $p_{j+1,k+1}$. and $p_{j+1,k-1}$ to make a centered-difference estimate of $\partial p/\partial\sigma$. $\hat{p}_{j,k}$ is estimated similarly, and then the PGF is estimated at $u_{j+1/2,k}$ by computing $\hat{p}_{j+1,k} - \hat{p}_{j,k}$.

At the lowest σ-level, $\sigma_K$, the standard PGF scheme extrapolates p from the $\sigma_K$ surface to the level $z_{j+1/2,K}$ by making a one-sided difference estimate of $\partial p/\partial\sigma$ (e.g., using $p_{j+1,K}$ and $p_{j+1,K-1}$ in Fig. 1) rather than a centered difference estimate.

## 3. ERROR ANALYSIS OF MM5'S PGF SCHEME

By expanding p in Taylor series with respect to σ and x, it is possible to estimate the leading truncation error terms for MM5's PGF scheme:

$$\frac{(\hat{p}_{j+1} - \hat{p}_j)}{\Delta x} = \left.\frac{\partial p}{\partial x}\right|_z + E_1 + E_2 + E_3 + \ldots$$

where $E_i$ are defined below. (In those expressions, $p^* \equiv p_0(z_s) - p_0(z_{top})$, where $p_0$ is basic-state pressure and $z_{top}$ is the height of the top-most σ-level.).

$E_1$ is $O(\Delta x^2)$. It arises from the centered difference estimate of the horizontal pressure gradient.

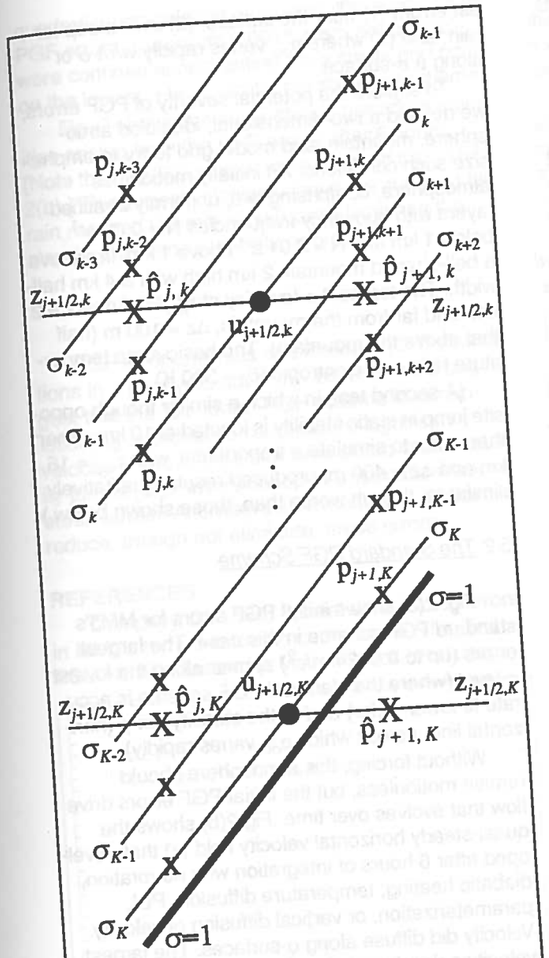


Figure 1. Vertical slice through a 2-D, staggered grid, showing σ-coordinate surfaces; perturbation pressures, p, at "X" points; two velocities, at dots: $u_{j+1/2,k}$ on the $\sigma_k$ level somewhere above the lowest σ-level, and $u_{j+1/2,K}$ on the lowest σ-level, $\sigma_K$; horizontal surfaces through each velocity point at altitudes $z_{j+1/2,k}$ and $z_{j+1/2,K}$, respectively; and estimated perturbation pressures, $\hat{p}$, at "X" points on each side of each velocity point on the z-surfaces. At the terrain surface, σ=1.

The quantity $(\partial z_s/\partial x)/(\Delta z/\Delta x)$ (where $\partial z_s/\partial x$ is the terrain slope and Δz and Δx are the vertical and horizontal grid resolutions, respectively) is relatively large in this case for illustration purposes, but not unrealistically large.

$$E_1 = \frac{1}{6}\left(\frac{\Delta x}{2}\right)^2 p_{xxx}\Big|_z$$

$$E_2 = -\frac{1}{2}\left(\frac{\Delta x}{2}\right)^2\left(\frac{\sigma_k p^*_x}{p^*}\right)^2 p_{\sigma\sigma x}\Big|_\sigma + \frac{1}{6}\left(\frac{\Delta x}{2}\right)^2\left(\frac{\sigma_k p^*_x}{p^*}\right)^3 p_{\sigma\sigma\sigma} - \frac{1}{2}\left(\frac{\Delta x}{2}\right)^2\left(\frac{\sigma_k}{p^*}\right)^2 (p^*_x p^*_{xx})(p_{\sigma\sigma}) - \frac{1}{6}(\sigma_{k+1} - \sigma_k)(\sigma_k - \sigma_{k-1})\left(\frac{\sigma_k}{p^*} p^*_x\right) p_{\sigma\sigma\sigma}$$

$$E_3 = \frac{1}{2}\left(\frac{\Delta x}{2}\right)^2\left(\frac{\sigma_k}{p^*}\right) p^*_{xx}\left[p_{\sigma x}\Big|_\sigma - \left(\frac{p^*_x}{p^*}\right) p_\sigma\right]$$

$E_2$ includes three terms of $O(\Delta x^2)$ and one of $O(\Delta\sigma^2)$. They arise from the vertical extrapolations of pressure from the $\sigma_k$-surface to the level, z, of the velocity point. The $O(\Delta\sigma^2)$ term arises from the centered difference estimate of $\partial p/\partial\sigma$. The $O(\Delta x^2)$ terms are all associated with the distance over which the vertical extrapolation of pressure must be performed. (The potential for partial cancellation of vertical interpolation errors when the difference $\hat{p}_{j+1} - \hat{p}_j$ is computed is responsible for some of the x-derivatives in all of these terms.)

$E_3$ is $O(\Delta x^2)$ and accounts for the error in estimating the level, z, of the velocity point.

At the lowest σ-level, $\sigma_K$, the leading terms are the same except for the $O(\Delta\sigma^2)$ term in $E_2$, which becomes $O(\Delta\sigma)$ and proportional to $p_{\sigma\sigma}$ rather than $p_{\sigma\sigma\sigma}$, as expected from a one-sided difference estimate of the vertical derivative.

All four terms in $E_2$ are proportional to some power of $\sigma_k p^*_x$ and therefore tend to be largest near the surface and where the terrain is most steeply sloped (since $p^*_x$ acts as a surrogate for the terrain slope).

Note that three of the four terms in $E_2$ do not diminish with higher vertical resolution (smaller$\Delta\sigma$) alone, an arguably undesirable property. This occurs because the distances over which vertical extrapolations must be performed do not diminish with decreasing Δσ, but rather with decreasing Δx.

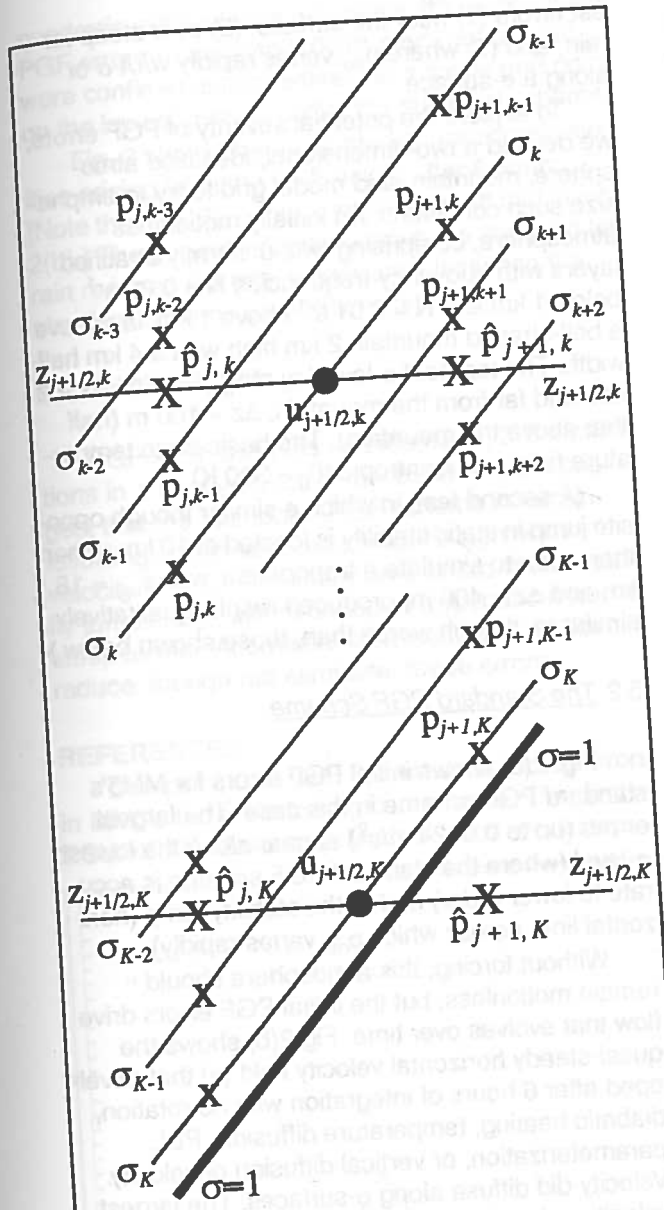


Figure 1. Vertical slice through a 2-D, staggered grid, showing σ-coordinate surfaces; perturbation pressures, p, at "X" points; two velocities, at dots: $u_{j+1/2,k}$ on the $\sigma_k$ level somewhere above the lowest σ-level, and $u_{j+1/2,K}$ on the lowest σ-level, $\sigma_K$; horizontal surfaces through each velocity point at altitudes $z_{j+1/2,k}$ and $z_{j+1/2,K}$, respectively; and estimated perturbation pressures, $\hat{p}$, at "X" points on each side of each velocity point on the z-surfaces. At the terrain surface, σ=1.

The quantity $(\partial z_s/\partial x)/(\Delta z/\Delta x)$ (where $\partial z_s/\partial x$ is the terrain slope and Δz and Δx are the vertical and horizontal grid resolutions, respectively) is relatively large in this case for illustration purposes, but not unrealistically large.

$$E_1 = \frac{1}{6}\left(\frac{\Delta x}{2}\right)^2 p_{xxx}\Big|_z$$

$$E_2 = -\frac{1}{2}\left(\frac{\Delta x}{2}\right)^2\left(\frac{\sigma_k p^*_x}{p^*}\right)^2 p_{\sigma\sigma x}\Big|_\sigma + \frac{1}{6}\left(\frac{\Delta x}{2}\right)^2\left(\frac{\sigma_k p^*_x}{p^*}\right)^3 p_{\sigma\sigma\sigma} - \frac{1}{2}\left(\frac{\Delta x}{2}\right)^2\left(\frac{\sigma_k}{p^*}\right)^2 (p^*_x p^*_{xx})(p_{\sigma\sigma}) - \frac{1}{6}(\sigma_{k+1}-\sigma_k)(\sigma_k-\sigma_{k-1})\left(\frac{\sigma_k}{p^*}p^*_x\right)p_{\sigma\sigma\sigma}$$

$$E_3 = \frac{1}{2}\left(\frac{\Delta x}{2}\right)^2\left(\frac{\sigma_k}{p^*}\right)p^*_{xx}\left[p_{\sigma x}\Big|_\sigma - \left(\frac{p^*_x}{p^*}\right)p_\sigma\right]$$

ence estimate of the horizontal pressure gradient.

$E_2$ includes three terms of $O(\Delta x^2)$ and one of $O(\Delta\sigma^2)$. They arise from the vertical extrapolations of pressure from the $\sigma_k$-surface to the level, z, of the velocity point. The $O(\Delta\sigma^2)$ term arises from the centered difference estimate of $\partial p/\partial\sigma$. The $O(\Delta x^2)$ terms are all associated with the distance over which the vertical extrapolation of pressure must be performed. (The potential for partial cancellation of vertical interpolation errors when the difference $\hat{p}_{j+1} - \hat{p}_j$ is computed is responsible for some of the x-derivatives in all of these terms.)

$E_3$ is $O(\Delta x^2)$ and accounts for the error in estimating the level, z, of the velocity point.

At the lowest σ-level, $\sigma_K$, the leading terms are the same except for the $O(\Delta\sigma^2)$ term in $E_2$, which becomes $O(\Delta\sigma)$ and proportional to $p_{\sigma\sigma}$ rather than $p_{\sigma\sigma\sigma}$, as expected from a one-sided difference estimate of the vertical derivative.

All four terms in $E_2$ are proportional to some power of $\sigma_k p^*_x$ and therefore tend to be largest near the surface and where the terrain is most steeply sloped (since $p^*_x$ acts as a surrogate for the terrain slope).

Note that three of the four terms in $E_2$ do not diminish with higher vertical resolution (smaller Δσ) alone, an arguably undesirable property. This occurs because the distances over which vertical extrapolations must be performed do not diminish with decreasing Δσ, but rather with decreasing Δx.

## 4. ERROR ANALYSES FOR OTHER SCHEMES

Mahrer (1984) described the most attractive alternative to the standard PGF scheme. In Mahrer's scheme, $\hat{p}_{j+1,k}$ and $\hat{p}_{j,k}$ in Fig. 1 are estimated wherever possible by interpolating p between σ-surfaces lying immediately above and below the level $z_{j+1/2,k}$, rather than extrapolating p vertically starting from $p_{j+1,k}$ and $p_{j,k}$, respectively, on the $\sigma_k$-surface. The leading error terms for Mahrer's scheme (employing linear interpolation w/ r/t σ) are the same as for MM5's standard scheme except for $E_2$, which becomes roughly

$$E_2 = \frac{(\Delta\sigma)^2}{8}(p_{\sigma\sigma})_x\Big|_z$$

(Mahrer's scheme with quadratic vertical interpolation is $O(\Delta\sigma^3)$ and proportional to $(p_{\sigma\sigma\sigma})_x|_z$.)

Note that this $E_2$ term does not depend on the terrain slope or on the σ-level, unlike $E_2$ for MM5's standard scheme. Moreover, it is entirely $O(\Delta\sigma^2)$, so it vanishes as Δσ does, a desirable property.

Unfortunately, Mahrer's scheme does not apply when a $\hat{p}$ must be estimated outside the model grid, as is usual for at least one of each pair of $\hat{p}$'s for velocities on the lowest σ-level (e.g., $\hat{p}_{j+1,K}$ in Fig. 1), and as is sometimes true at higher σ-levels, too. Such cases require extrapolation of p outside the model grid*. No generally optimal method is known, though some methods may work better than others in a given context. Possibilities include:

(1) one-sided, vertical, linear extrapolation (part of the standard scheme);

(2) one-sided, quadratic extrapolation; and

(3) horizontal extrapolation (at constant z).

The errors of all schemes depend formally not only on the Δσ and Δx, but also on the spatial distribution of perturbation pressure, p. The choice of basic state affects this distribution, but no single reference state can be generally optimal.

## 5. TESTS OF SOME PGF SCHEMES

### 5.1 *A Test Case*

The error analysis in section 3 suggests that the standard PGF scheme might produce the largest errors (1) near the surface; (2) over steep terrain; and (3) where $p_{\sigma\sigma}$ varies rapidly w/r/t σ or along a σ-surface.

To explore the potential severity of PGF errors, we defined a two-dimensional, idealized atmosphere, mountain, and model grid to try to emphasize such conditions. An initially motionless atmosphere, comprising two, uniformly stratified layers with buoyancy frequencies N = 0.02 $s^{-1}$ below 1 km and N = 0.01 $s^{-1}$ above 1 km, lay above a bell-shaped mountain 2 km high with a 4 km half-width. The topmost σ-level lay at $z_{top}$ = 4 km. Δx = 2 km, and far from the mountain, Δz = 100 m (half that above the mountain). The basic-state temperature field was isentropic ($\theta_0$ = 300 K).

(A second test, in which a similar though opposite jump in static stability is located at 10 km rather than 1 km to simulate a tropopause, with $z_{top}$ = 16 km and Δz = 400 m, produced results qualitatively similar to, though worse than, those shown below.)

### 5.2 *The Standard PGF Scheme*

Fig. 2(a) shows initial PGF errors for MM5's standard PGF scheme in this case. The largest errors (up to 0.0024 m/$s^2$) appear along the lowest σ-level (where the standard PGF scheme is accurate to lower order) and at the stability jump (horizontal line, across which $p_{\sigma\sigma}$ varies rapidly).

Without forcing, this atmosphere should remain motionless, but the initial PGF errors drive flow that evolves over time. Fig 2(b) shows the quasi-steady horizontal velocity field (u) that developed after 6 hours of integration with no rotation, diabatic heating, temperature diffusion, PBL parameterization, or vertical diffusion of velocity. Velocity did diffuse along σ-surfaces. The largest velocities developed near the steepest terrain slopes and exceeded 5 m/s, a significant error by most standards. The spurious velocities were strongly sheared just above the surface, so adding large, explicit vertical diffusion of velocity reduced the maximum velocity errors by an order of magnitude, but this arbitrary "solution" may have unintended consequences if applied in general.

### 5.3 *An Alternative PGF Scheme*

Of the ten PGF schemes that we analyzed, the best in this test case (taking into account initial PGF errors, subsequent velocity errors, stability, and ease of coding), was Mahrer's scheme with quadratic, vertical interpolation when possible, and quadratic extrapolation otherwise. It's largest initial PGF errors (maximum 0.0018 m/$s^2$, not shown) were confined almost entirely to a single grid point on the lowest σ-level, unlike the standard scheme.

Fig. 3 shows the quasi-steady horizontal velocities arising from the PGF errors after 6 hours. [Note that Fig. 3's contour interval is half that in Fig. 2(b).] The largest velocities above the steepest terrain reached 0.8 m/s, significantly less than the standard scheme's velocity errors.

## 6. CONCLUSIONS

PGF error analyses and idealized, 2-D simulations in a nonhydrostatic, mesoscale model suggest that the "standard" PGF scheme in terrain-following coordinates can produce significant velocity errors in slow flow near sharp static stability jumps (e.g., inversion top or tropopause) above steep terrain. Alternative schemes can significantly reduce, though not eliminate, these errors.

## REFERENCES


Dempsey, D., 1996. Spatial-differencing errors in MM5's terrain-following coordinates. The Sixth PSU/NCAR Mesoscale Model Users' Workshop.

Dudhia, J., 1993. A nonhydrostatic version of the Penn State-NCAR Mesoscale Model: Validation Tests and Simulation of an Atlantic Cyclone and Cold Front. *Mon. Wea. Rev.* **121**, 1493-1513.

Mahrer, Y., 1984. An improved numerical approximation of the horizontal gradients in a terrain-following coordinate system. *Mon. Wea. Rev.* **112**, 918-922





Figure 2(a). Initial PGF errors for the "standard" PGF scheme in MM5. (Cont. int: 2x$10^{-4}$ m/$s^2$. Max. error: 2.4x$10^{-3}$ m/$s^2$). Bell-shaped mountain 2 km high with 4 km half-width. Motionless atmosphere, with N = 0.02 $s^{-1}$ below 1 km (horizontal line) and 0.01 $s^{-1}$ above. Isentropic, hydrostatic basic-state temperature ($\theta_0$ = 300 K). Δx = 2 km; Δz = 100 m far from mountain; $z_{top}$ = 4 km.

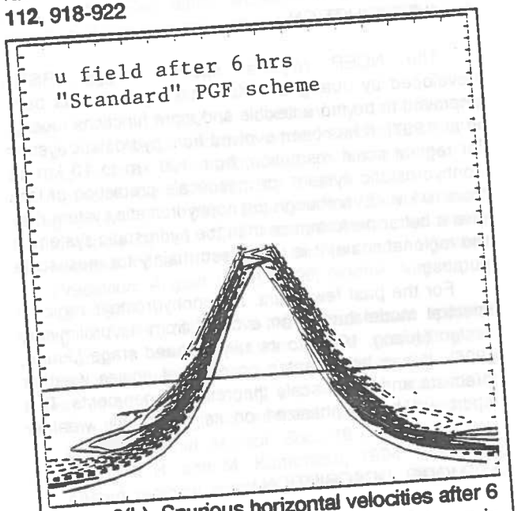


Figure 2(b). Spurious horizontal velocities after 6 hour integration using "standard" PGF scheme in MM5. Cont. interval: 0.5 m/s. Max. error: 5 m/s.




Figure 3. Spurious horizontal velocities after 6 hour integration using Mahrer's PGF scheme with quadratic, vertical interpolation of perturbation pressure when possible, quadratic extrapolation otherwise. Cont. int.: 0.25 m/s. Max. err.: 0.8 m/s.

*Unless terrain is assumed to be step-shaped, as, for example, in NCEP's eta model. Then u = 0, avoiding any need to estimate the PGF but introducing other, possibly undesirable consequences.

quadratic extrapolation otherwise. It's largest initial PGF errors (maximum 0.0018 m/s$^2$, not shown) were confined almost entirely to a single grid point on the lowest $\sigma$-level, unlike the standard scheme.

Fig. 3 shows the quasi-steady horizontal velocities arising from the PGF errors after 6 hours. [Note that Fig. 3's contour interval is half that in Fig. 2(b).] The largest velocities above the steepest terrain reached 0.8 m/s, significantly less than the standard scheme's velocity errors.

## 6. CONCLUSIONS

PGF error analyses and idealized, 2-D simulations in a nonhydrostatic, mesoscale model suggest that the "standard" PGF scheme in terrain-following coordinates can produce significant velocity errors in slow flow near sharp static stability jumps (e.g., inversion top or tropopause) above steep terrain. Alternative schemes can significantly reduce, though not eliminate, these errors.

## REFERENCES


Dempsey, D., 1996. Spatial-differencing errors in MM5's terrain-following coordinates. The Sixth PSU/NCAR Mesoscale Model Users' Workshop.

Dudhia, J., 1993. A nonhydrostatic version of the Penn State-NCAR Mesoscale Model: Validation Tests and Simulation of an Atlantic Cyclone and Cold Front. *Mon. Wea. Rev.* **121**, 1493-1513.

Mahrer, Y., 1984. An improved numerical approximation of the horizontal gradients in a terrain-following coordinate system. *Mon. Wea. Rev.* **112**, 918-922


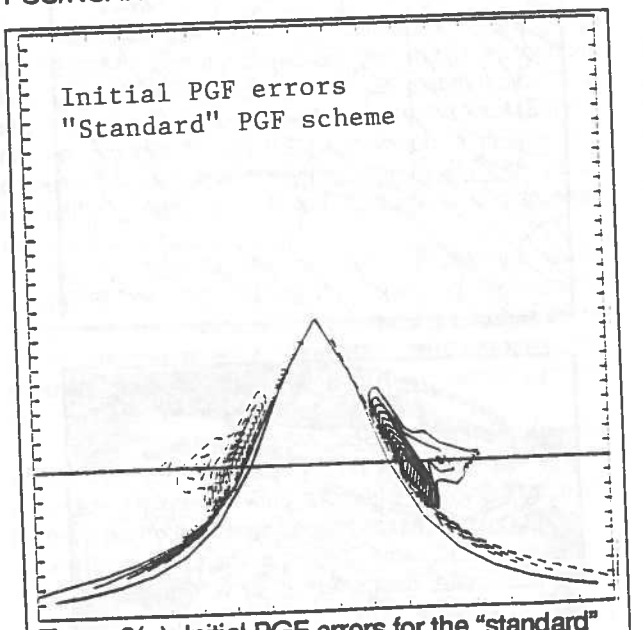


Figure 2(a). Initial PGF errors for the "standard" PGF scheme in MM5. (Cont. int: 2x10$^{-4}$ m/s$^2$. Max. error: 2.4x10$^{-3}$ m/s$^2$). Bell-shaped mountain 2 km high with 4 km half-width. Motionless atmosphere, with N = 0.02 s$^{-1}$ below 1 km (horizontal line) and 0.01 s$^{-1}$ above. Isentropic, hydrostatic basic-state temperature ($\theta_0$ = 300 K). $\Delta x$ = 2 km; $\Delta z$ = 100 m far from mountain; $z_{top}$ = 4 km.

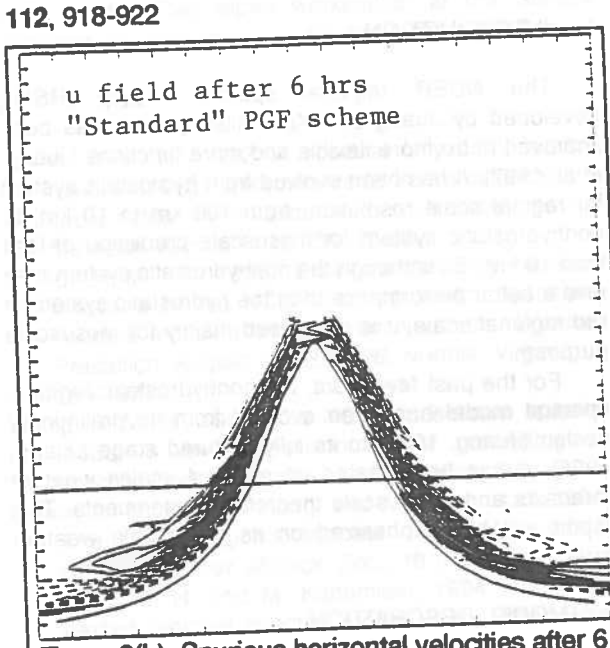


Figure 2(b). Spurious horizontal velocities after 6 hour integration using "standard" PGF scheme in MM5. Cont. interval: 0.5 m/s. Max. error: 5 m/s.

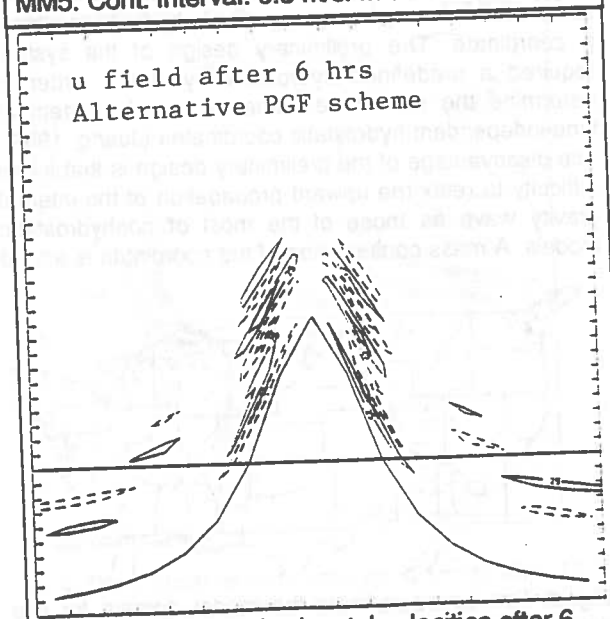


Figure 3. Spurious horizontal velocities after 6 hour integration using Mahrer's PGF scheme with quadratic, vertical interpolation of perturbation pressure when possible, quadratic extrapolation otherwise. Cont. int.: 0.25 m/s. Max. err.: 0.8 m/s.